

Variational Interpolation of Circulation with Nonlinear, Advective Smoothing*

G. G. PANTELEEV⁺

Department of Physics and Physical Oceanography, Memorial University of Newfoundland, St. John's, Newfoundland, Canada

N. A. MAXIMENKO⁺

International Pacific Research Center, University of Hawaii at Manoa, Honolulu, Hawaii

B. DEYOUNG

Department of Physics and Physical Oceanography, Memorial University of Newfoundland, St. John's, Newfoundland, Canada

C. REISS

Department of Biological Sciences, Old Dominion University, Norfolk, Virginia

T. YAMAGATA

Department of Earth and Planetary Science, University of Tokyo, Tokyo, Japan

(Manuscript received 16 November 1999, in final form 27 November 2001)

ABSTRACT

A modified variational algorithm, previously proposed in meteorology, is presented for the interpolation of oceanic hydrographic and velocity data. The technique is anisotropic and involves a variational approach that allows revealing of the spatial structure in its application. Being a part of the variational family of algorithms, the method is quite general in that it allows one to set dynamical constraints, and weighting functions, applicable to the problem of interest. This flexibility is illustrated by using the nonlinear terms of momentum balance equation as constraints. The inclusion of these constraints appears to assist in the resolution of narrow jets in the flow fields. The method is applied to data from two different regions of the ocean: Lagrangian drifter data from the northwest Pacific and hydrographic data from the Scotian Shelf. Each dataset presents quite different scales, physical processes, and data types. The resulting flow fields are compared with results determined from traditional optimal interpolation, and advantages of the proposed method are discussed.

1. Introduction

Over the past decades variational methods have been shown to have clear advantages compared to statistical methods for several different types of problems. Sasaki (1955, 1958, 1970) was the first to propose the application of variational principles rather than optimal interpolation for objective analysis (Gandin 1965). Different variational algorithms have been successfully ap-

plied in meteorology (e.g., Lewis 1972; Penenko and Obraztsov 1976; Navon 1981). Code for some of these algorithms is available for application (Legler and Navon 1991).

Despite their formal difference, statistical and variational methods have the same origin. Both are based on the least squares method of fitting model to data. McIntosh (1990) has shown that when the correlation function is known in theory, the optimal interpolation method (Gandin 1965) is preferred. In general, however, the correlation is not known in theory and is often difficult to estimate, even in practice. This means that the correlation function often has to be estimated, or guessed. The variational interpolation method should give smaller errors in interpolation, as it is less sensitive to the chosen correlation space scale. It is probably this feature of the variational method that guarantees successful application of the variational approach for rather different problems (Navon 1981; Hoffman 1984; Legler

* School of Ocean and Earth Science Technology Contribution Number 5947, and International Pacific Research Center Contribution Number 147.

⁺ Additional affiliation: Shirshov Institute of Oceanography, Moscow, Russia.

Corresponding author address: Dr. Brad deYoung, Physics and Physical Oceanography, Memorial University of Newfoundland, St. John's, NF A1B 3X7, Canada.
E-mail: bdeyoung@physics.mun.ca

et al. 1989; Pantelev and Yaremchuk 1989). The key advantage of these variational algorithms is that they can explicitly include dynamical constraints in the interpolation algorithm.

An increase in computational power and the opportunity for optimal assimilation of different sources of the data stimulated development of three dimensional algorithms based on the variational principles. These algorithms were found to be very useful in operational meteorology. For example, both the European Centre for Medium-Range Weather Forecasts (ECMWF) and the National Centers for Environmental Prediction (NCEP) use a 3D variational technique for reanalysis (Pu et al. 1997). Application of three dimensional variational interpolation schemes helped to define the structure of the large-scale circulation in the Labrador Sea (Provost and Salmon 1986) and mesoscale currents in the northwest Pacific (Pantelev 1990).

The application of the technique of optimal control (Le Dimet and Talagrand 1986) permits the inclusion of more complicated time-dependent dynamical constraints (Griffin and Thompson 1996; Nechaev and Yaremchuk 1994; Nechaev et al. 1997) in the interpolation scheme. Unfortunately, the proper use of optimal control and three-dimensional variational techniques requires not only large amounts of data and their uniform distribution in space, but that the data must also correspond with the appropriate dynamical constraints. In the absence of sufficient corresponding data, these methods became ill-conditioned and can provide false results, because a substantial number of degrees of freedom defined by their constraints remain undefined. Such a situation is quite common in oceanography, where extensive three dimensional and time-dependent observations are difficult to obtain.

At the same time, the underlying dynamics of many oceanic problems can be identified even if the observed oceanic circulation is often quite complex. In such a case, it seems natural to specify the length and/or time-scales for the dominant processes and create an algorithm appropriate for the available data. Variational objective analysis of the pseudostress over the Indian Ocean carried out by Legler et al. (1989) (see also Ramamurthy and Navon 1992) and mesoscale velocity fields observed in the northwest Pacific during the summer of 1987 (Pantelev and Yaremchuk 1989) are examples.

Here, we present a relatively simple two-dimensional variational algorithm that we use to stimulate the upper-layer ocean circulation. Although rather similar to the methods proposed by Legler et al. (1989) and Pantelev and Yaremchuk (1989), it also has some differences that allow the inference of anisotropy in the interpolated velocity fields. This feature could be quite useful in some applications. As an illustration, we applied the proposed algorithm in two situations: 1) the definition of the surface circulation in the northwest Pacific based on the drifter measurements and 2) the definition of the

surface circulation on the Scotian Shelf from “estimates” of the upper-layer currents, using dynamical velocities determined from density profiles.

2. Variational algorithm

To define the stationary, upper-layer circulation from estimates of horizontal velocities given on an irregular grid, we search for a two-dimensional velocity field that minimizes the function \mathbf{F} that is the sum of the individual constraints for the problem:

$$\mathbf{F} = \sum_{i=1}^4 \mathbf{f}_i, \quad (1)$$

where \mathbf{f}_i defines some “weak” (according to Sasaki 1970) constraints:

$$\mathbf{f}_1 = \int_{\Omega} (u_{xx}^2 + u_{yy}^2 + v_{xx}^2 + v_{yy}^2)/g_1(x, y) d\Omega, \quad (2)$$

$$\mathbf{f}_2 = \int_{\Omega} (\nabla \mathbf{u})^2/g_2(x, y) d\Omega, \quad (3)$$

$$\mathbf{f}_3 = \sum_{n=1}^N (\mathbf{A}\mathbf{u} - \mathbf{u}_n^*)^2/g_3(x_n, y_n), \quad (4)$$

$$\mathbf{f}_4 = \int_{\Omega} [(uu_x + vv_y)^2 + (uv_x + vu_y)^2]/g_4(x, y) d\Omega. \quad (5)$$

Here, Ω is a space domain and $g_i(x, y)$ are components of the weight function. A linear operator \mathbf{A} matches the solution to observed velocities. Most of the constraints, Eqs. (2)–(5), are similar to ones used by Legler et al. (1989) and Pantelev and Yaremchuk (1989).

The first constraint (2) brings smoothness to the modeled velocity field and essentially defines the spatial scale of the velocity field. Although Eq. (2) is not invariant to rotation, this form for the smoothness term is commonly used because of its simplicity (Thacker 1988; Nechaev et al. 1997).

The second term, Eq. (3), is a kinematic constraint that forces the resulting velocity field to be nondivergent. Although horizontal velocities may converge in the upper mixed layer, for instance because of a non-uniform wind stress field or isopycnal motions at baroclinic fronts outcropping at the sea surface, the corresponding 3D circulation plays a secondary role and is composed of ageostrophic velocities, which are typically much weaker than geostrophic ones (e.g., Uchida et al. 1998). The third term naturally expresses the attraction to the original data and provides a major input into the algorithm.

The last term minimizes the nonlinear terms of the momentum equation and has rather clear mathematical and physical meaning. It is proportional to the along-stream velocity gradient, and its minimization is equivalent to the application of an anisotropic smoother. This

feature of \mathbf{f}_4 is particularly useful in the description of narrow meandering jets and their smoothing without creating large errors in the cross-jet scales and absolute values of the velocities. From the physical point of view, the minimization of \mathbf{f}_4 decreases the ageostrophic velocity component, which, according to results of Le Traon and Hernandez (1992), Ichikawa et al. (1995), Sheng and Thompson (1996), and others, is weak at the mesoscale.

The choice of the weight functions g_i is a key step in the application of the method. According to the standard formalism of the least squares model of fitting data (Thacker 1988, 1989), the minimum of \mathbf{F} will correspond to the most probable state, whereas the weights g_i represent the covariances of the corresponding physical values. We believe that all the fields are δ -correlated with unknown means, so the weight functions g_i become the error covariance of these fields. Thus, the best statistical knowledge will provide the most probable state that can be obtained under the chosen constraints and available data.

If the statistics are unknown, we need to define the weight function g_i based upon prior experience and physical intuition. Usually such knowledge can only capture the principal features; therefore, it seems logical to conduct numerical experiments to see if the model outcome fits sensibly with our assumptions.

We introduce the weights g_i as

$$g_1(x, y) = [\mathbf{U}(x, y)/\mathbf{L}^2(x, y)]^2/k_1, \quad (6)$$

$$g_2(x, y) = [\mathbf{U}(x, y)\varepsilon_{\text{div}}(x, y)/\mathbf{L}(x, y)]^2/k_2, \quad (7)$$

$$g_3(x, y) = [\mathbf{U}(x, y)\varepsilon_{\text{data}}(x, y)]^2/k_3, \quad (8)$$

$$g_4(x, y) = [\mathbf{U}^2(x, y)/\mathbf{L}(x, y)]^2/k_4, \quad (9)$$

where \mathbf{U} and \mathbf{L} are characteristic velocity and spatial scales, ε_{div} is the nondivergence error, ranging between 0.05 and 0.1 (Pantelev and Yaremchuk 1989), and $\varepsilon_{\text{data}}$ is the prior data error. Because of subjectivity in the definition of \mathbf{U} and \mathbf{L} , we incorporate additional coefficients, k_i , and assume that the correct choice of k_i has to provide integral errors,

$$\sigma_{\text{div}} = \left[4 \int_{\Omega} (\nabla \mathbf{u})^2 d\Omega \div \int_{\Omega} (u_x^2 + u_y^2 + v_x^2 + v_y^2) d\Omega \right]^{0.5}, \quad (10)$$

$$\sigma_{\text{data}} = \left[\sum_{n=1}^N (\mathbf{u} - \mathbf{u}_n^*)^2 / \sum_{n=1}^N (\mathbf{u}_n^*)^2 \right]^{0.5}, \quad \text{and} \quad (11)$$

$$\sigma_{\text{ageos}} = \text{rms}[(\mathbf{u}\nabla)\mathbf{u}]/\text{rms}(\mathbf{f}\mathbf{u}), \quad (12)$$

in agreement with our physical knowledge. As will be shown later, the proposed variational algorithm is rather insensitive to reasonable changes, by up to two orders

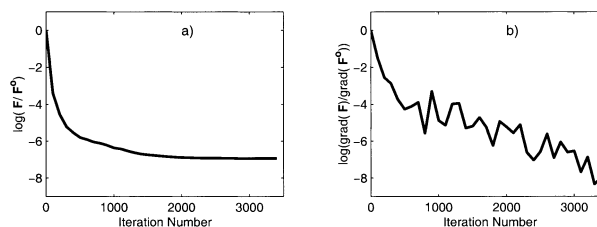


FIG. 1. (a) The variation of the scaled functional \mathbf{F} with respect to the number of iterations. (b) The variation of the scaled gradient with respect to the number of iterations.

of magnitude, in k_i . This lack of sensitivity is consistent with McIntosh (1990), mentioned in the introduction.

The finite-difference analog of \mathbf{F} was expressed in spherical coordinates on a C grid (Messinger and Arakawa 1976). The rigid boundaries were taken into account by adding zero velocity “data” for the points occupied by the Asian continent and different islands. These data were incorporated into \mathbf{f}_3 with a correspondingly large weight, g_i . For the minimization of \mathbf{F} , a limited memory quasi-Newtonian large-scale algorithm was applied (Gilbert and Lemarechal 1989).

We illustrate the proposed algorithm using two examples. In the first, we were interested in the large-scale, surface circulation of the northwest Pacific Ocean estimated using surface drifters. In the second, we seek to determine the surface current on the Nova Scotia shelf from a large-scale hydrographic survey.

The dimension of the control vector was about 21 000 and 4500 for the data from the northwest Pacific and the Scotian Shelf, respectively. It typically took about 3000 iterations to reach the functional minimum in the first case, although in Fig. 1 we can see that most of the convergence to the minimum is achieved after 1000 iterations. For the second case, the minimum is reached after about 300–500 iterations.

The relatively large number [in comparison with Ramamurthy and Navon (1992)] of iterations required to reach the minimum may have several different causes. Relative to the work of Ramamurthy and Navon, the most probable reason for the relatively slow convergence here is the different form of the minimized function (1) and the cost function utilized by Ramamurthy and Navon (1992). They included an additional smoothed climate velocity field that substantially enhances convergence to the minimum. Our numerical experiments showed that the introduction of a similar “attractor” to the climate velocity field in our algorithm allowed us to accelerate convergence by about 10 times.

Another potential factor in the slow convergence here is the nonlinearity of constraint (4) and the irregularity of the weight function g_3 , which is chosen to be much larger over continental land than over the ocean. The nonlinearity can make the cost function very irregular, while the second term is likely to slow the minimization algorithm.

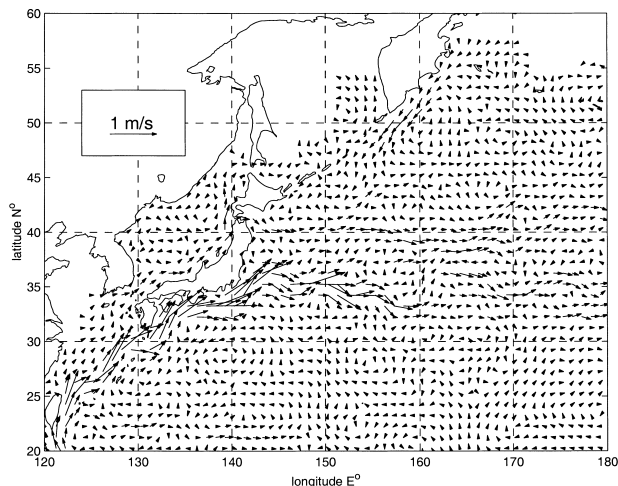


FIG. 2. The surface velocity field in the northwest Pacific derived by the variational method from the drifter data. Velocities are plotted on a 1°N, 1°E grid.

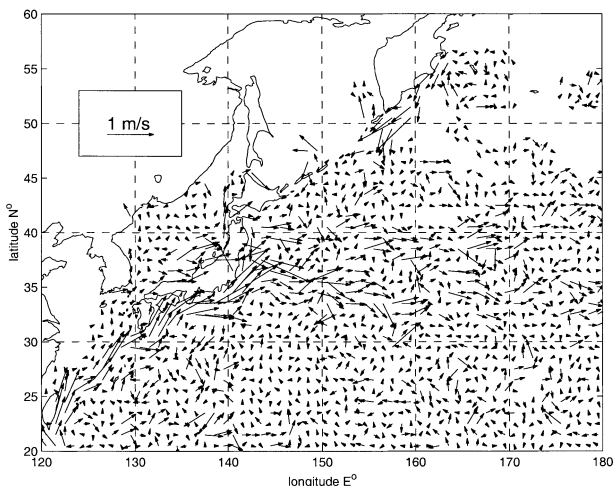


FIG. 3. Surface velocity field in the northwest Pacific averaged over 1°N, 1°E boxes.

3. Surface circulation in the northwest Pacific

a. Data

The data available for the northwest Pacific consisted of 296 Lagrangian drifters deployed between 1987 and 1996. The initial processing of these data was accomplished by the National Oceanographic and Atmospheric Administration (NOAA) Atlantic Oceanographic and Meteorological Laboratory (AOML). Drifter data were quality controlled and optimally interpolated to 6-h interval trajectories (Hansen and Poulain 1996). As velocity input, \mathbf{u}_i^* , we used the mean velocity of all drifters in 0.5°N, 0.5°E boxes. The constraint function \mathbf{F} was also defined on the same grid.

b. Choice of parameters

For the horizontal space scale \mathbf{L} we chose the baroclinic Rossby radius $\mathbf{L}(x, y) = N(x, y) * H(x, y)/f(y)$ calculated from the Levitus (1982) climatology. Here $N(x, y)$ is the Brunt–Väisälä frequency, $H(x, y)$ the ocean depth, and $f(y)$ the Coriolis parameter. The internal Rossby deformation scale \mathbf{L} changes gradually from 200 km in the southern regions to 50 km in the north and in shallow regions. The scale $\mathbf{U}(x, y)$ was initially estimated as the mean velocity scale in 2.5°N, 2.5°E boxes and interpolated onto a 0.5°N, 0.5°E grid by using the optimal interpolation method with a Gaussian correlation function whose correlation scale was 400 km. Then the sequence of the application of the technique described above was completed by updating $\mathbf{U}(x, y)$ in each iteration from the previous iteration result.

The value $\varepsilon_{\text{div}}(x, y)$ was defined as 0.1. We believe that $\varepsilon_{\text{data}}(x_n, y_n)$ is proportional to $(M_{ij})^{1/2}$, where M_{ij} is the number of drifters in the i - j th box of the grid. The values of k_i were chosen to yield $\sigma_{\text{div}} = 0.11$, $\sigma_{\text{ageos}} = 0.025$, and $\sigma_{\text{data}} = 0.45$. The values of σ_{ageos} and σ_{div}

follow from the balance of the Coriolis and nonlinear terms in the momentum equation and analysis of geostrophic and ageostrophic currents in the surface (Uchida et al. 1998). In our further discussion, we will refer to the values k_i , which provide σ_{div} , σ_{data} , and σ_{ageos} , corresponding to our physical understanding as “optimal.”

c. Results

The mean mixed layer velocity field computed with the proposed variational technique (Fig. 2) contains all the primary known features of the large-scale circulation in the northwest Pacific. A comparison with results from simple spatial averaging of the same data within 1°N, 1°E bins (Fig. 3) reveals the advantage of the proposed algorithm. The primary currents seen in Fig. 2 are: the Subtropical Countercurrent, flowing eastward along 22°–23°N east of Taiwan; the Kuroshio Current with a set of its quasi-stationary meanders and recirculations trapped by the shoreline shape and bottom topography; the eastward-flowing Kuroshio Extension with its perturbations developing and decaying downstream; the Tsushima Current, flowing along the west coast of Japan after separation from the Kuroshio southwest of Kyushu; the Kamchatka Current, flowing southwestward along the east coast of the Kamchatka Peninsula; and the subarctic front jet flowing along 40°N and interacting in a complex way with the Kuroshio Extension. It is remarkable that some drifters outlining this jet originate in the Japan Sea through the Tsugaru Strait (Maximenko et al. 1997). Very unclear or even missing in Fig. 2 are the Kurill and Oyashio Currents. Their absence from the data is probably explained by the limited drifter statistics north of 42°N (Maximenko et al. 1997). The same insufficient data make doubtful the flow pattern in the subpolar gyre and in the Sea of Okhotsk. Compared to Fig. 3, the flow pattern in Fig.

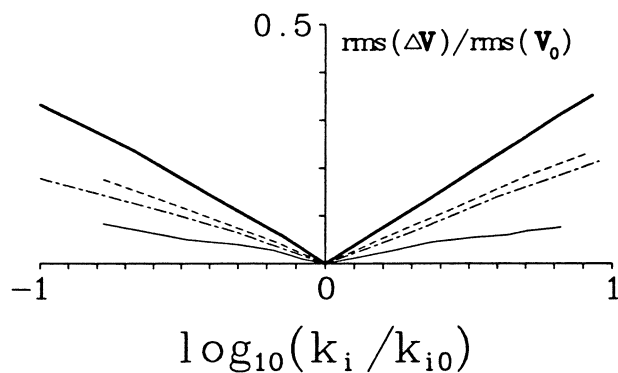


FIG. 4. The sensitivity of the variational solution to changes in the coefficients k_1 (smoothness; dashed line), k_2 (divergence; thin solid line), k_3 (data; thick solid line), and k_4 (nonlinearity, dash-dotted line).

2 is much less noisy in the interior of the subtropical gyre, where relatively weak currents form a number of vortices of various size and sign. These vortices are seen in original data and may be a surface manifestation of multiple subgyres (Wijffels et al. 1998).

Comparison of Figs. 2 and 3 suggests that the gaps or holes in the distribution of drifter data in space are not critical for the interpolation. For example, an absence of the data in the region with coordinates 42°N and 161°E (Fig. 3) does not prevent a realistic eastward current corresponding to the subarctic front jet along 40°N (Fig. 2). Of course, an absence of data in a region means that the any result within that region is not reliable. For this reason, we do not plot the velocity field in the Sea of Okhotsk or the China Sea.

As described earlier, the choice of k_i has some subjective features. Nevertheless, moderate (up to one to two orders of magnitude) changes in k_i relative to the “optimal” value k_i^o have small effects on the resulting fields (Fig. 4). Changes in k_3 (responsible for data-counterparts matching) naturally had the greatest influence on the difference final solution.

As an exploration of why our algorithm requires a relatively large number of iterations to find the minimum of the cost function, we plot the difference between velocity fields obtained after the 2500th and 2000th iterations (Fig. 5). During the final stage of the minimization processes, adjustment to the optimal solution takes place mostly in the regions with relatively strong and complicated current structure, such as the Kuroshio Extension, and the Kamchatka and Tsushima Currents, where the nonlinear constraint (4) is essential. Thus, it appears, not surprisingly perhaps, that the nonlinear terms are regulating the rate of convergence in this problem.

4. Surface circulation on the Nova Scotia shelf

a. Data

Between 20 November and 2 December 1997, a large-scale CTD survey was conducted on the central and

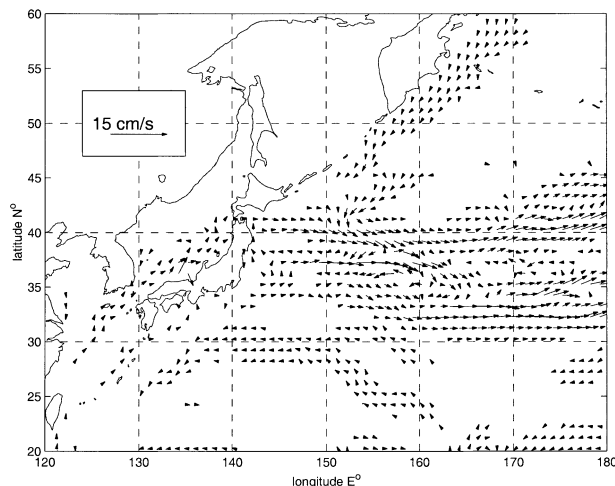


FIG. 5. The difference between the velocity fields obtained after the 2500th and 2000th iterations of the minimization algorithm. Note the change in the velocity scale from Figs. 2 and 3.

eastern Scotian Shelf. The survey consisted of 95 stations and covered a region about $200\text{ km} \times 400\text{ km}$, with a typical station separation of about 25 km. Because changes in bottom density along isobaths were small, it was possible to calculate the dynamic height using the method of Sheng and Thompson (1996), with velocity calculated relative to 250 m. These dynamic heights permitted estimation of the velocity projection perpendicular to a line connecting any two points. We also had direct velocity measurements at five current meters located at four mooring stations on Western Bank (Fig. 8). These current measurements were used only as an independent measure of interpolation quality and were not used as data inputs to the variational calculation.

b. Choice of parameters

According to Sheng and Thompson (1996) and Griffin and Thompson (1996), the circulation on the Scotian Shelf is closely related to bottom topography and can be described as a series of currents concentrated near the shelf slope and the offshore marine banks. The typical subtidal velocities and their spatial correlation scale are about $U = 15\text{ cm s}^{-1}$ and $L_1 = 35\text{--}45\text{ km}$, respectively. Approximately the same value for the optimal correlation radius R was determined by varying R to obtain the best match between direct measurements from the four current meters and the velocity field obtained using the optimal interpolation method with a Gaussian correlation function

$$S(r) = \exp[-(r^2/R^2)]. \quad (13)$$

Figure 6 shows that the best correspondence between the optimally interpolated field and the measured velocity data, with a fairly clear and strong minimum, occurs at a correlation length scale (R) of 33 km. These

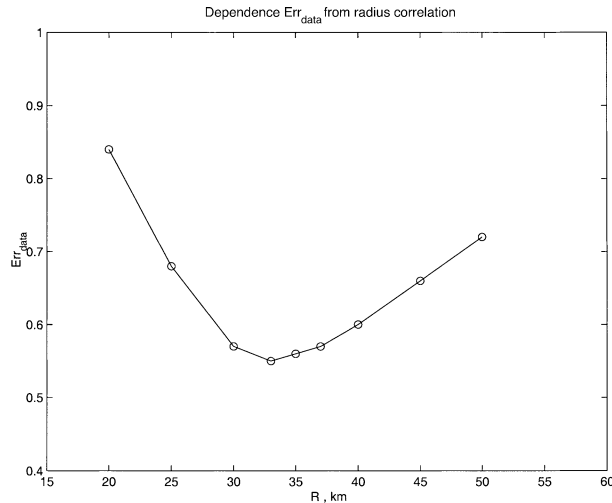


FIG. 6. The dispersion of the measured and optimal interpolated velocities from the four mooring stations as a function of correlation radius R .

values were used to define g_2 , g_3 , and g_4 , as in Eqs. (6)–(9). At the same time, taking into account the steep topography along some parts of the shelf and in order to avoid oversmoothing, we introduced a smaller space scale, $L_2 = 20$ km, as the scale where the degree of isotropy should be large. We use the scale L_2 instead of L_1 in the definitions of g_1 and g_4 [(6)–(9)], believing that where the topography is steep there is more influence of the dynamical constraints. The nondivergence error ε_{div} was estimated as 0.1, and $\varepsilon_{\text{data}}$ was defined as

$$\varepsilon_{\text{data}}^n = 0.2 + 0.2(R_n/L_2), \quad (14)$$

where R_n is the distance between two dynamic height estimates (we used only pairs of points where the distance $\leq L_1$).

The horizontal scale of the grid was about 7 km in the zonal and 8 km in the meridional direction. The optimal choice of k_i provided $\sigma_{\text{div}} = 0.07$, $\sigma_{\text{data}} = 0.38$, and $\sigma_{\text{ageos}} = 0.03$. According to (14), we expect to obtain σ_{data} of about 0.3. So, a σ_{data} value of 0.38 is probably somewhat large. This may arise because of changes in the bottom density along isobaths in the northeast corner of Western Bank, hence violating one of our assumptions, and errors in our choice of the zero velocity level. A similar result was found by Sheng and Thompson (1996; see their Fig. 11) for the same area of the Scotian Shelf.

c. Results

We calculated the velocity fields using the variational method and the optimal interpolation method with a Gaussian correlation function (13), $R = 33$ km (Figs. 7a,b). Comparison of the two figures shows that the variational method has some clear advantages in velocity interpolation near the coastline and around islands.

Furthermore, the absolute value of the current velocity as calculated by the optimal interpolation method is greater than that calculated using the variational algorithm. The variational algorithm decreased some of the unrealistic local current intensification in the northeast part of our study area. This intensification is probably connected with changes in bottom density along isobaths, leading to inconsistencies in our application of the dynamic method in this region.

Comparisons with direct measurements from the four current meters at 40-m (the northern mooring) and 24-m (other moorings) depth shows the advantages of the variational algorithm more objectively (Figs. 8a,b). The errors between the measured and the calculated velocities are lower for the variational algorithm (44%) than for the optimal interpolation method (55%).

Note that the velocity optimal interpolation velocity field does not contain any information about the circulation north of Western Bank. At the same time, the variational algorithm produces currents similar to the measured data and to currents obtained by diagnostic calculations in the Western Bank region (Fig. 8c) obtained by using a primitive equation model (Semenov and Luneva 1996).

5. Discussion and conclusions

The variational approach (Wunsch 1996) allows calculation of error estimates of the interpolated fields (i.e., velocity errors in our algorithm). The natural way to obtain these errors is to calculate and invert the Hessian,

$$\mathbf{H}_{i,j} = (\nabla_{u+\delta u_i} \mathbf{F} - \nabla_{u-\delta u_i} \mathbf{F})_j / 2\delta u_i, \quad (15)$$

in the vicinity of the optimal state. There are a number of ways to calculate the Hessian matrix (Schroter 1989; Thacker 1989; Zou et al. 1992), but it is rather difficult to invert because of the enormous number of independent variables. It is possible, however, to calculate the largest λ_{max} and smallest λ_{min} eigenvalues of the Hessian matrix by using the iterative power method and shifted power iteration approach (see Zou et al. 1992). Such computations may provide useful information about the Hessian matrix, for example, its condition number $\lambda_{\text{max}}/\lambda_{\text{min}}$.

Following Zou et al. (1992), we estimated pairs of $(\lambda_{\text{max}}, \lambda_{\text{min}})$ as $(3.17 \times 10^6, 2.5)$ and $(362.81, 1.09 \times 10^{-2})$ for the first (northwestern Pacific) and second (Scotian Shelf) examples described in this paper. The corresponding condition numbers are 1.26×10^6 and 3.32×10^4 .

The FORTRAN code of our algorithm is written with single (six decimals) precision accuracy. The smallest eigenvalue in the first case is probably overestimated, and is in fact indistinguishable from zero, because of roundoff errors that develop when the shifted power iteration method is applied. The eigenmodes associated with the small eigenvalues of the first case are lost in the numerical noise of the solution. In spite of the range

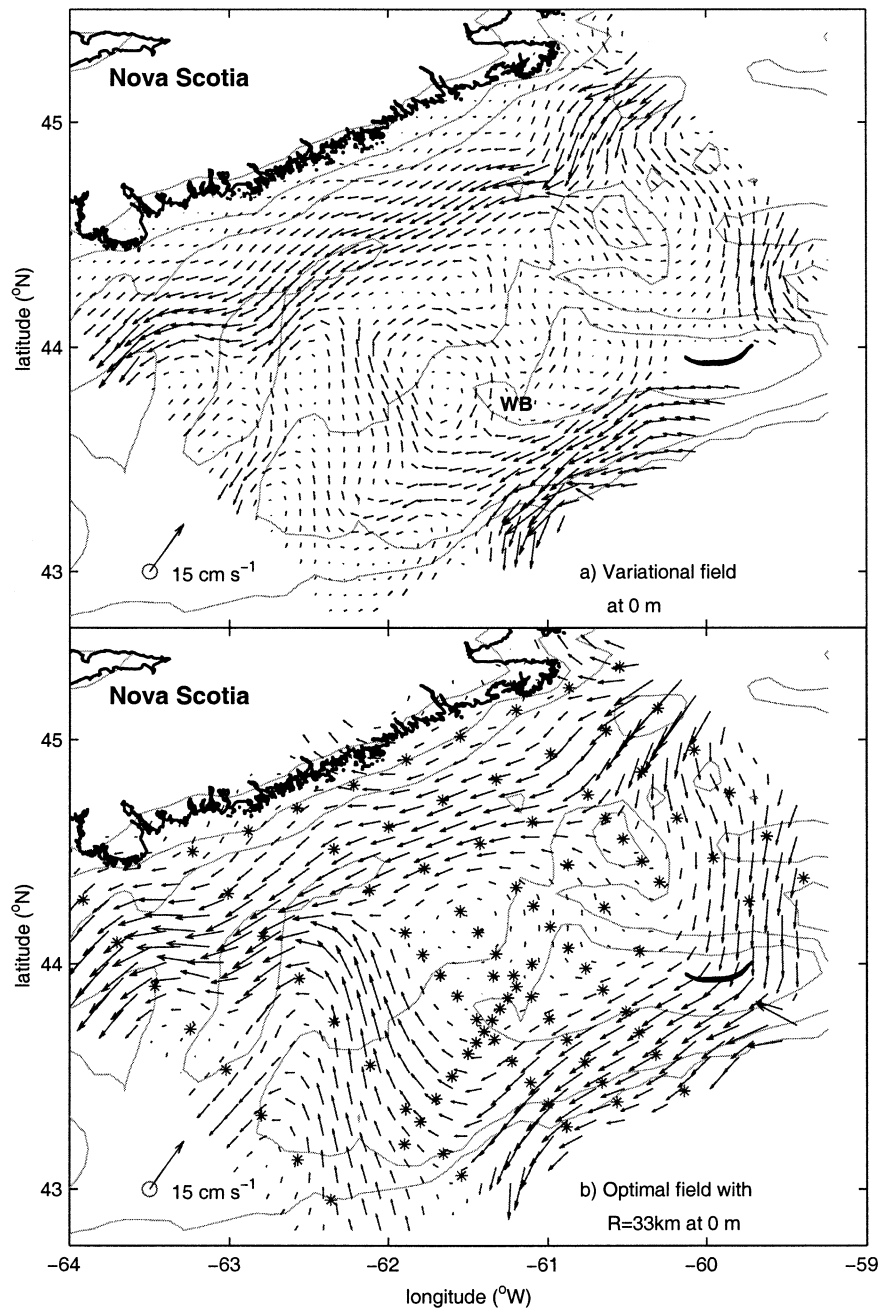


FIG. 7. The velocity field in the Scotian Shelf as calculated using (a) the variational method and (b) the optimal interpolation method with the correlation function given by Eq. (13) and $R = 33$ km.

of eigenvalues, the search algorithm is still able to locate the optimal solution to the problem (see Fig. 1).

The proposed variational algorithm has some clear advantages over the traditional optimal interpolation method. The primary advantage is the opportunity to explicitly include information on the dynamical characteristics of the problem, through use of the constraint functions f_1 and f_4 , whose minimizations have clear mathematical and physical meaning. We showed, with

two very different examples, the power of this technique in representing spatial structure. In particular, application of a constraint representing an anisotropic smoothing function allows us to better represent the detailed features of jets both on the shelf and in the open ocean.

Within this anisotropic interpolation problem it is possible to include terms to represent previously known space scales. The algorithm also permits additional dynamical information to be incorporated into the solution.

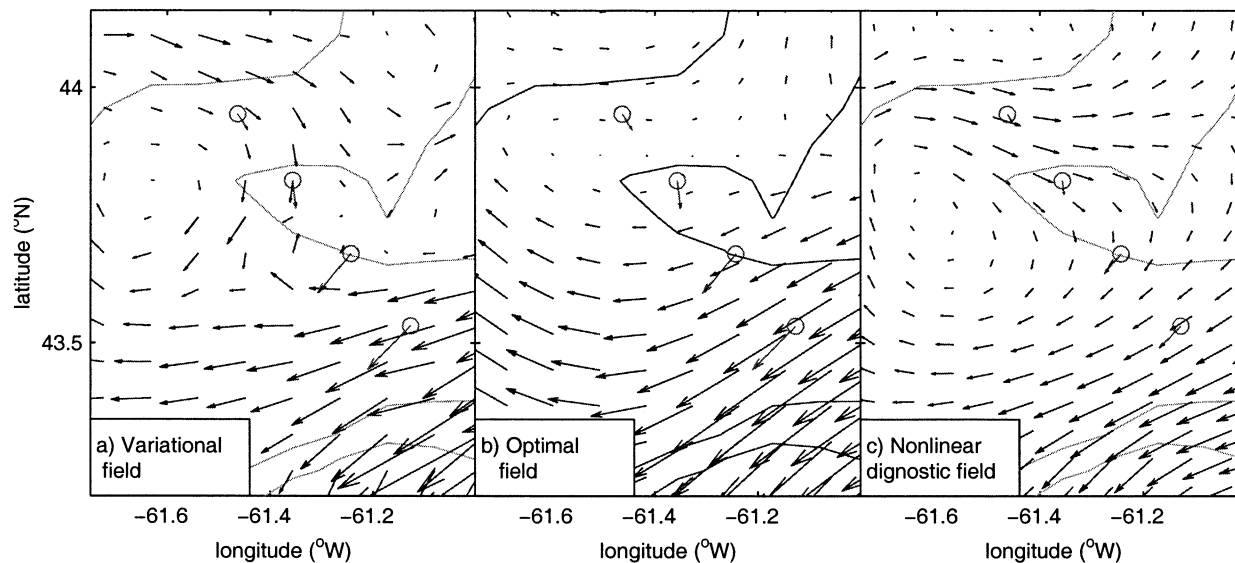


FIG. 8. (a), (b) Same as in Fig. 5, but for the Western Bank region. Also shown is the location of four mooring stations and the dispersion of measured and calculated velocities. (c) The result of diagnostic calculations with a primitive equation model.

The great practical difficulty lies in the definition of the weight functions g_i . As for the constraints, these weights could have been defined differently, although we found that the final results depend only weakly on the choice of the weighting functions g_i .

Acknowledgments. We thank the Global Drifter Center, Scripps Institution of Oceanography, and Atlantic Oceanographic and Meteorology Laboratory for the krieged drifter dataset from the western North Pacific provided for this study. This research was supported by an NSERC grant, through GLOBEC Canada to BdeY, and also by the Frontier Research System for Global Change (to NM).

REFERENCES

- Gandin, L. S., 1965: *Objective Analysis of Meteorological Fields*. Israel Program for Scientific Translation, 242 pp.
- Gilbert, J. C., and C. Lemarechal, 1989: Some numerical experiments with variable storage quasi-Newton algorithms. *Math. Prog.*, **45**, 407–455.
- Griffin, D. A., and K. R. Thompson, 1996: The adjoint method of data assimilation used operationally for shelf circulation. *J. Geophys. Res.*, **101**, 3457–3477.
- Hansen, D. V., and P.-M. Poulain, 1996: Quality control and interpolations of WOCE–TOGA drifter data. *J. Atmos. Oceanic Technol.*, **13**, 900–909.
- Hoffman, R., 1984: SASS wind ambiguity removal by direct minimization. Part II: Use of smoothness and dynamical constraints. *Mon. Wea. Rev.*, **112**, 1829–1852.
- Ichikawa, K., S. Imawaki, and H. Ishii, 1995: Comparison of surface velocities determined from altimeter and drifting buoy data. *J. Oceanogr.*, **51**, 729–740.
- Le Dimet, J. M., and O. Talagrand, 1986: Variational algorithms for analysis and assimilation of meteorological observations: Theoretical aspects. *Tellus*, **38A**, 97–110.
- Legler, D. M., and I. M. Navon, 1991: VARIATM—A FORTRAN code for objective analysis of pseudo-stress with large-scale conjugate-gradient minimization. *Comput. Geosci.*, **17**, 1–21.
- , —, and J. J. O'Brien, 1989: Objective analysis of pseudo-stress over the Indian Ocean using a direct minimization approach. *Mon. Wea. Rev.*, **117**, 709–720.
- Le Traon, P.-Y., and F. Hernandez, 1992: Mapping the oceanic mesoscale circulation: Validation of satellite altimetry using surface drifters. *J. Atmos. Oceanic Technol.*, **9**, 687–698.
- Levitus, S., 1982: *Climatological Atlas of the World Ocean*. NOAA Prof Paper 13, 173 pp. and 17 microfiche.
- Lewis, J. M., 1972: The operational analysis using the variational method. *Tellus*, **24**, 514–530.
- Maximenko, N., G. Pantelev, A. Grotov, P. P. Niller, and T. Yamagata, 1997: Mean circulation in the north western Pacific mixed layer from TOGA/WOCE Lagrangian drifters. *Proc. Second CREAMS Int. Symp.*, Fukuoka, Japan, Research Institute for Applied Mechanics, Kyushu University, 189–192.
- McIntosh, P. C., 1990: Oceanographic data interpolation: Objective analysis and splines. *J. Geophys. Res.*, **95**, 13 529–13 541.
- Mesinger, F., and A. Arakawa, 1976: *Numerical Methods Used in Atmospheric Models*. GARP Publication Series 17, Vol. 1, WMO, 64 pp.
- Navon, I. M., 1981: Implementation of a posteriori methods for enforcing conservation of potential enstrophy and mass in discretized shallow-water equation models. *Mon. Wea. Rev.*, **109**, 946–958.
- Nechaev, D. A., and M. I. Yaremchuk, 1994: Application of adjoint technique to processing of a standard section data set: WOCE section S4 along 67S in the Pacific Ocean. *J. Geophys. Res.*, **100**, 865–879.
- , G. G. Pantelev, and M. I. Yaremchuk, 1997: The circulation in the Amundsen and Bellingshausen Seas from atmospheric and oceanic climatic data. *Oceanology*, **37** (5), 586–594.
- Pantelev, G. G., 1990: Three-dimensional variational method for interpolation of ocean velocity field. *Oceanology*, **30** (4), 495–498.
- , and M. I. Yaremchuk, 1989: Two methods for interpolation of data from measurements of the current velocity at autonomous buoy stations. *Oceanology*, **29** (3), 400–405.
- Penenko, V. V., and N. N. Obratcov, 1976: The variational method for initialization of meteorological-element fields. *Meteor. Gidrol.*, **11**, 3–16.

- Provost, C., and R. Salmon, 1986: A variational method for inverting hydrographic data. *J. Mar. Res.*, **44**, 1–24.
- Pu, Z.-X., E. Kalnay, D. Parrish, W. Wu, and Z. Toth, 1997: The use of bred vectors in the NCEP Global 3D Variational Analysis System. *Wea. Forecasting*, **12**, 689–695.
- Ramamurthy, M. K., and I. M. Navon, 1992: The conjugate–gradient variational analysis and initialization method: An application to MONEX SOP-2 data. *Mon. Wea. Rev.*, **120**, 2360–2377.
- Sasaki, Y. K., 1955: A fundamental study of the numerical prediction based on the variational principle. *J. Meteor. Soc. Japan*, **33**, 262–275.
- , 1958: An objective analysis based on the variational method. *J. Meteor. Soc. Japan*, **36**, 77–88.
- , 1970: Some basic formalism in numerical variational analysis. *Mon. Wea. Rev.*, **98**, 738–742.
- Schroter, J., 1989: Driving of nonlinear time dependent ocean models by observation of transient tracers—A problem of constrained optimization. *Oceanic Circulation Models: Combining Data and Dynamics*. D. L. Anderson and J. Willebrand, Eds., Kluwer Academic, 257–285.
- Semenov, E. V., and M. V. Luneva, 1996: Numerical model for tidal and density driven circulation of the White Sea. *Izv. Akad. Navk SSSR, Phys. Atmos. Ocean*, **32**, 704–713.
- Sheng, J., and K. R. Thompson, 1996: A robust method for diagnosing regional shelf circulation from scattered density profiles. *J. Geophys. Res.*, **101**, 25 647–25 659.
- Thacker, W. C., 1988: Fitting models to inadequate data by enforcing spatial and temporal smoothing. *J. Geophys. Res.*, **93**, 10 655–10 665.
- , 1989: The role of Hessian matrix in fitting models to data. *J. Geophys. Res.*, **94**, 1227–1240.
- Uchida, H., S. Imawaki, and J.-H. Hu, 1998: Comparison of Kuroshio surface velocities derived from satellite altimeter and drifting buoy data. *J. Oceanogr.*, **54** (1), 115–122.
- Wijffels, S. E., M. M. Hall, T. Joyce, D. J. Torres, P. Hacker, and E. Firing, 1998: Multiple deep gyres of the western North Pacific: A WOCE section along 149 degrees E. *J. Geophys. Res.*, **103**, 12 985–13 009.
- Wunsch, C., 1996: *The Ocean Circulation Inverse Problem*. Cambridge University Press, 442 pp.
- Zou, X., I. M. Navon, and F. X. Le Dimet, 1992: Incomplete observations and control of gravity waves in variational data assimilation. *Tellus*, **44A**, 273–296.